

# Contrast edge colors under different natural illuminations

Juan Luis Nieves,<sup>1,\*</sup> Sérgio M. C. Nascimento,<sup>2</sup> and Javier Romero<sup>1</sup>

<sup>1</sup>*Department of Optics, University of Granada, 18071 Granada, Spain*

<sup>2</sup>*Centre of Physics, University of Minho, 4710-057 Braga, Portugal*

\*Corresponding author: jnieves@ugr.es

Received September 1, 2011; revised December 8, 2011; accepted December 8, 2011;  
posted December 12, 2011 (Doc. ID 153746); published January 27, 2012

Essential to sensory processing in the human visual system is natural illumination, which can vary considerably not only across space but also along the day depending on the atmospheric conditions and the sun's position in the sky. In this work, edges derived from the three postreceptoral Luminance, Red–Green, and Blue–Yellow signals were computed from hyperspectral images of natural scenes rendered with daylights of Correlated Color Temperatures (CCTs) from 2735 to 25,889 K; for low CCT, the same analysis was performed using Planckian illuminants up to 800 K. It was found that average luminance and chromatic edge contrasts were maximal for low correlated color temperatures and almost constants above 10,000 K. The magnitude of these contrast changes was, however, only about 2% across the tested daylights. Results suggest that the postreceptoral opponent and nonopponent color vision mechanisms produce almost constant responses for color edge detection under natural illumination. © 2012 Optical Society of America

OCIS Codes: 330.1720, 330.1690.

## 1. INTRODUCTION

Object colors depend on both the spectral reflectance of the surfaces and the spectral power distribution (SPD) of the light impinging on them. It has been argued that our human visual system is adapted to natural stimuli to code and process efficiently the visual inputs it receives [1]. An example of that efficient sensory processing is how color vision has evolved in response to natural image regularities, which include the color and luminance distributions across images, the power spectra of natural images, among others [2]. Essential to that sensory processing is natural illumination, which can vary considerably not only across space but also throughout the day, depending on the atmospheric conditions and on the sun's position in the sky [3–5]. Optimization in natural image processing usually consists of first-order statistics (just looking at a single image pixel), second-order statistics (capturing relations and regularities over pairs of image pixels in the image), or higher-order statistics (referring to any kind of transformation or analysis involving more than two pixels) [6]. All of these statistical models applied to natural images assume that one of the major roles of human vision is to represent visual information in an optimal way, i.e., to eliminate redundant information.

The distribution of luminance, color, and local contrast in natural scenes has been quantitatively and qualitatively described comprehensively (for a review, see [7]). Correlations among receptor cone responses are usually found by virtue of the close overlap in the cones' spectral sensitivities. But the three postreceptoral responses, here referred to as Red–Green (RG), Blue–Yellow (BY), and Luminance (Lum) channels, decorrelate the cone signals to remove information in the cone outputs that is redundant. Higher-order representations and structures (e.g., edges and contours) have similar mathematical properties and sometimes redundancy can be a reliable indicator of material boundaries [8]. Some authors have

recently evaluated contrast and color edge statistics to test whether the aforementioned statistical approaches also hold at a second stage of color vision. Zhou and Mel [9] used different color images to compute edges along the RG, BY, and Lum components of those images. They found that most edges were defined by luminance contrast with color information being redundant. More recently, Hansen and Gegenfurtner [10] studied the correlation between luminance and color contrasts for edges in natural images and found that they were almost independent of each other. However, if one ignores the sign of contrast change across the edge in order to represent higher-order image structure, i.e., to determine whether color and luminance edges tend to co-occur, color and luminance are not independent but positively correlated [8]. Although some authors have concluded from this that color is redundant [9], this is not the case; for example, illumination boundaries such as shading and shadows tend to be defined by luminance not color contrast [8]. Thus, in scenes with dense foliage, which tend to be replete with shadows and shading, the detection of, for example, RG variations becomes important for the detection of objects such as fruit [11–12].

The purpose of this work was to study how changes in daylight illumination affect the edges in color images. Although image gradients and their distributions have also been analyzed for natural images [10,13], limited data are available concerning the chromatic edge contrast deviations across natural illuminant changes. Edge colors were computed from different hyperspectral images of natural scenes rendered with daylights of Correlated Color Temperatures (CCTs) from 2735 to 25,889 K and were analyzed for the Lum, RG, and BY signals.

## 2. METHODS

### A. Dataset

The analysis was based on hyperspectral images of nine scenes representing landscapes and nonurban scenarios

[14–15]. The scenes consisted of a mixture of rural scenes from the Minho region of Portugal, containing, rocks, trees, leaves, grass, and earth and from the cities of Porto and Braga, Portugal (see Fig. 1). The estimated reflectance spectra (effective spectral reflectance) at each pixel were sampled in 10 nm steps over 400–700 nm. All images were acquired under daylight and, for the estimation of the spectral reflectances, the illumination was assumed to be spatially uniform. Analysis of the effects of shadows on the estimation of effective spectral reflectances for surfaces under direct and indirect illumination can be found in [16], where it is demonstrated that, under ideal conditions (that is, discarding the effects of the geometrical position of the sun), the estimations of the color signals in shadows and directly illuminated conditions can be safely done under the aforementioned assumptions.

The hyperspectral images were rendered under 108 SPDs of daylights with CCTs from 2735 to 25,889 K (see Fig. 1). [If the chromaticity of a light source is off the Planckian locus, the CCT is used instead of color temperature to describe its appearance. Let us suppose that  $(x_1, y_1)$  is the chromaticity of an off-locus light source. By definition, the CCT of  $(x_1, y_1)$  is the temperature of the Planckian radiator whose chromaticity is nearest to  $(x_1, y_1)$ .] The illuminant set was comprised by two different kinds of SPDs: a real dataset and a simulated dataset. The real daylight SPDs were measured in Granada, Spain, from sunrise to sunset under different atmospheric conditions and covering a vast range of CCTs from 4800 up to 30,000 K [3]. The simulated daylight SPDs were obtained with SBDART, a software tool to compute plane-parallel radiative transfer energy in clear and cloudy conditions within the Earth's atmosphere and at the surface [17] to cover CCTs below 4800 K. The chromaticity coordinates of Granada daylight lie far above the CIE locus at high CCTs ( $>9000$  K), and a CCT of 5700 K best typifies this daylight.

## B. Cones and Postreceptoral Responses

The color signal at each image pixel (product of the spectral reflectance at a pixel by the SPD of the illumination) was transformed to LMS cone values using the Smith and Pokorny cone sensitivities [18] according to

$$\begin{aligned} L &= \sum_{\lambda=400}^{700} l(\lambda)r(\lambda)e(\lambda)\Delta\lambda, \\ M &= \sum_{\lambda=400}^{700} m(\lambda)r(\lambda)e(\lambda)\Delta\lambda, \\ S &= \sum_{\lambda=400}^{700} s(\lambda)r(\lambda)e(\lambda)\Delta\lambda, \end{aligned} \quad (1)$$

where  $\lambda$  is the wavelength,  $l$ ,  $m$ , and  $s$  are the cone sensitivities,  $r$  is the spectral reflectance, and  $e$  the SPD of the illuminant (all the spectral functions were sampled using  $\Delta\lambda = 10$  nm).

Next, each LMS image was transformed into a postreceptoral signal, which was composed of one Lum and two opponent, RG and BY, signals. Different definitions of color-opponent responses can be found in the color vision literature, either based on biologically neural representations (e.g., [19]), statistical analysis of postreceptoral responses (e.g., [20–21], among others) or even in terms of cone contrast

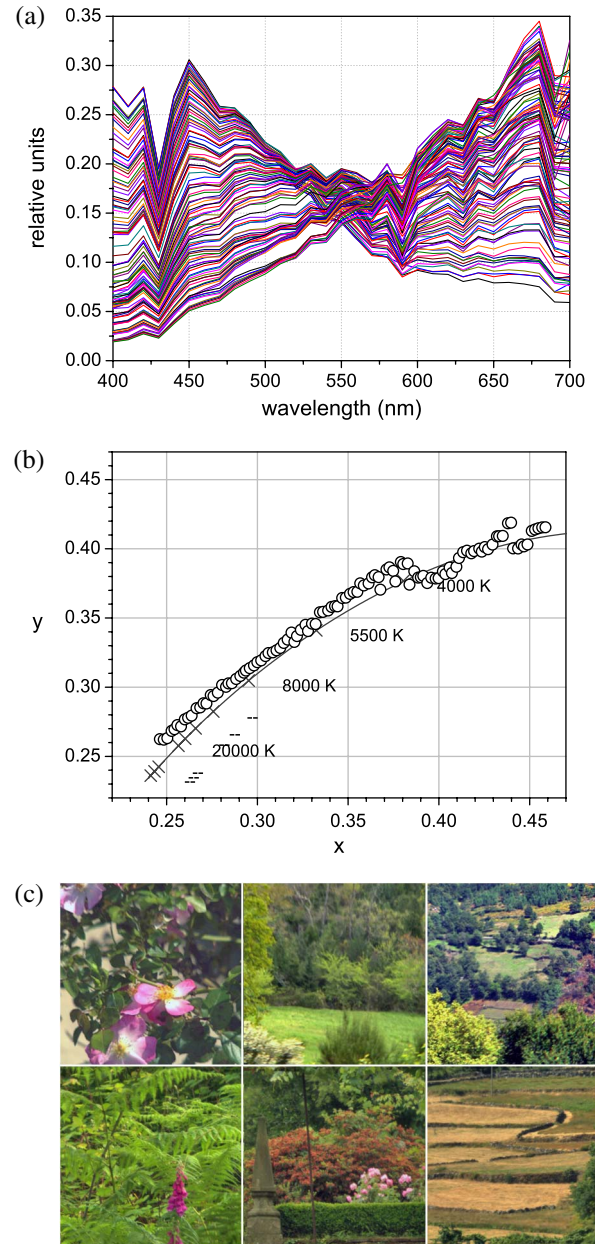


Fig. 1. (Color online) (a) SPDs for daylights of correlated color temperatures between 2735 and 25,889 K. (b) The CIE 1931  $x, y$  chromaticities of the daylight spectra (open circles) overlaid with the Planckian locus (solid line). (c) Examples of the natural scenes that are used for the experiment.

(e.g., [22]). The following transformations of the LMS cone excitations were used here [20]:

$$\begin{aligned} \text{Lum} &= L + M, \\ \text{RG} &= L - M, \\ \text{BY} &= 2S - (L + M). \end{aligned} \quad (2)$$

## C. Edge Computation

The postreceptoral images were blurred using a Gaussian filter with a standard deviation of  $\sigma = 1$ , before performing edge computations to avoid artifacts in the image data. Figure 2 shows an example of the color-opponent edge computation.

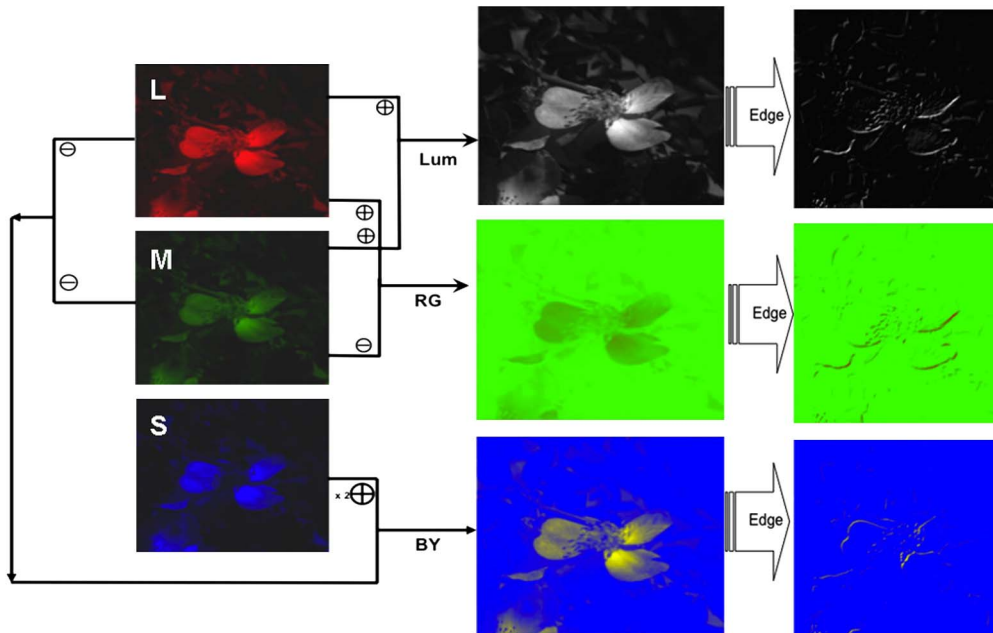


Fig. 2. (Color online) Overview of the color-opponent edge computation. A hyperspectral image was rendered under each of the daylights and (left column) the three  $L$ ,  $M$ , and  $S$  cone planes were obtained; (middle column) the postreceptoral Lum, RG, and BY images were computed, and (right column) edges were detected in each image. All the image planes are shown here in false color.

The edges across the Lum, RG, and BY image planes were detected using a Sobel operator [10]. Mathematically, the Sobel operator uses a  $3 \times 3$  filter to calculate approximations to the first derivative in the horizontal  $h$  and vertical  $v$  directions as

$$E_k^h = \begin{pmatrix} -1 & 0 & 1 \\ -2 & 0 & 2 \\ -1 & 0 & 1 \end{pmatrix} * I_k; \quad E_k^v = (E_k^h)^T, \quad (3)$$

where  $k$  represents the Lum, RG, and BY components,  $I_k$  is the source image for the  $k$ th component,  $E_k^h$  and  $E_k^v$  the two images that at each point contain the horizontal and vertical derivative approximations, and  $*$  and  $T$  denote convolution and transpose, respectively. At each point in the image, the resulting gradient approximations can be combined to a gradient magnitude by averaging in order to obtain the final  $k$ th edge image  $E_k$  estimation

$$E_k = \frac{1}{2}(E_k^h + E_k^v). \quad (4)$$

### 3. RESULTS

#### A. Influence of Illuminant Changes on the Chromatic and Luminance Edges

To investigate the influence of daylight changes on the chromatic and luminance edges, we computed the average of edge differences across pairs of illuminants. For each natural image, all the possible combinations of edges detected under two different daylights were computed for the Lum, RG, and BY channels at a pixel. The average statistics quantify how daylight changes influence edge detection and are shown in Table 1. The edge differences were greater for a pair of extreme daylight conditions (i.e., a hypothetical observer moving from a reddish ambient daylight around 2700 K to a bluish

ambient daylight around 30,000 K) than for a pair of daylights with intermediate CCTs.

#### B. Examining Edge Contrasts across Changes in Daylight

Apart from the average statistics, another important measure of image statistics is the marginal distribution of contrasts (i.e., the probability distribution of the variables contained in the subset of all contrast values). The importance of contrast in vision is suggested, for instance, by neurophysiological findings, which reveal the lateral inhibition mediated by neurons. Apart from that, also by psychophysical experiments that show how perceived brightness of objects is mainly determined by the surrounding context, i.e., the average local contrast between the objects and the background [23]. We computed the luminance and chromatic edge contrast for the  $i$ th illuminant and  $j$ th scene as the ratio between the absolute values of the gradient and the source image at a pixel  $x$  as

$$C_{i,j,k}^x = \frac{|\nabla E_{i,j,k}^x|}{I_{i,j,k}^x}, \quad (5)$$

where  $k$  represents the Lum, RG, and BY color components. For each image, the edge contrasts were averaged across all image pixels to obtain the final average edge contrast as

**Table 1. Average Statistics for Edge Differences Among All Possible Pairs of Illuminants from 2,735 to 25,889 K<sup>a</sup>**

	Lum	RG	BY
<b>Min</b>	$-5.6e-07$	$3.1e-07$	$-7.2e-05$
<b>Max</b>	$7.1e-05$	$3.9e-05$	$5.5e-07$
<b>Mean</b>	$4.3e-05$	$2.6e-05$	$-4.4e-05$
<b>Median</b>	$4.3e-05$	$2.9e-05$	$-4.3e-05$
<b>Standard deviation</b>	$1.7e-05$	$1.0e-05$	$1.7e-05$

<sup>a</sup>Results were averaged for all the pixels and natural scenes used.

$$\overline{C_{i,k}} = \frac{1}{9} \sum_{j=1}^9 \left( \frac{1}{N} \sum_{x=1}^N C_{i,j,k}^x \right), \quad (6)$$

where  $N$  stands for the total amount of pixels in the  $j$ th scene.

According to the previous results, it is reasonable to assume that, as daylight changes, the magnitude of the gradients also changes. Figure 3 shows examples of the results for the average magnitude of the contrast for three different daylights. The marginal distributions of gradients across daylights show how the number of occurrences along the nonopponent and opponent color mechanisms decreases as the edge contrasts increases. This is similar to the results found by previous studies on a log scale [9,13]. There were no considerable differences among the results obtained for the  $k$ th different color vision mechanisms. It can be seen that the similarity of the results holds at low contrast values where the distribution of edge contrasts falls almost linearly; however, for intermediate and high contrast values (above 0.4 edge contrasts) marginal distributions are observed to be more different.

Besides marginal distributions of contrasts, we also looked at average edge contrast across the daylight range. Figure 4 illustrates the chromatic and luminance edge contrast changes across illuminants for the three color vision mechanisms. The figure shows two different variations of the average edge contrasts common to the Lum, RG, and BY color vision systems: on one hand, for relative low daylight, CCT edge contrasts markedly changed and decreased up to 9000 K; on the other hand, for high daylight CCT above 10,000 K, the edge contrasts were almost constant for the three mechanisms. But the magnitude of the contrast change varied only around 2% from the maximum edge contrast across all the daylights studied; the change was only of 1% for the RG channel and close to 3% for the Lum channel. Results suggest that the opponent and nonopponent color vision mechanisms tend to lead constant responses for color edge detection under natural illumination, with the RG system being much more stable and efficient at such task.

So, are the maximum edge contrast values for the three channels a global maximum across natural illumination? The answer should be yes, if we consider only daylight. But what can we predict for illuminants with CCT below the daylight CCTs? Although we cannot simulate real daylights with CCTs below 2700 K, we performed the same analysis but using 10 SPDs of Planckian illuminants with CCTs running from 800 up to 2600 K (i.e., clearly below the natural limit for daylights). Figure 5 shows the average chromatic and luminance edge contrasts obtained when the hyperspectral images were rendered under those nonnatural illuminations. The magnitude of the contrast rate change was around 2.5% on average, slightly greater than the one obtained for the natural daylights, and the general trend was also almost the same; the Lum and BY systems were again more unstable under illuminant changes for edge detection.

### C. Edge Contrasts for Adapted Receptor Responses

Color constancy is usually defined as a stable color perception under different illumination conditions [24]. Among the variety of cues to color constancy and the several forms it can manifest are the context and image statistics. Correlations between Lum and “redness” within the retinal image can be exploited as a cue to the chromatic properties of illuminants

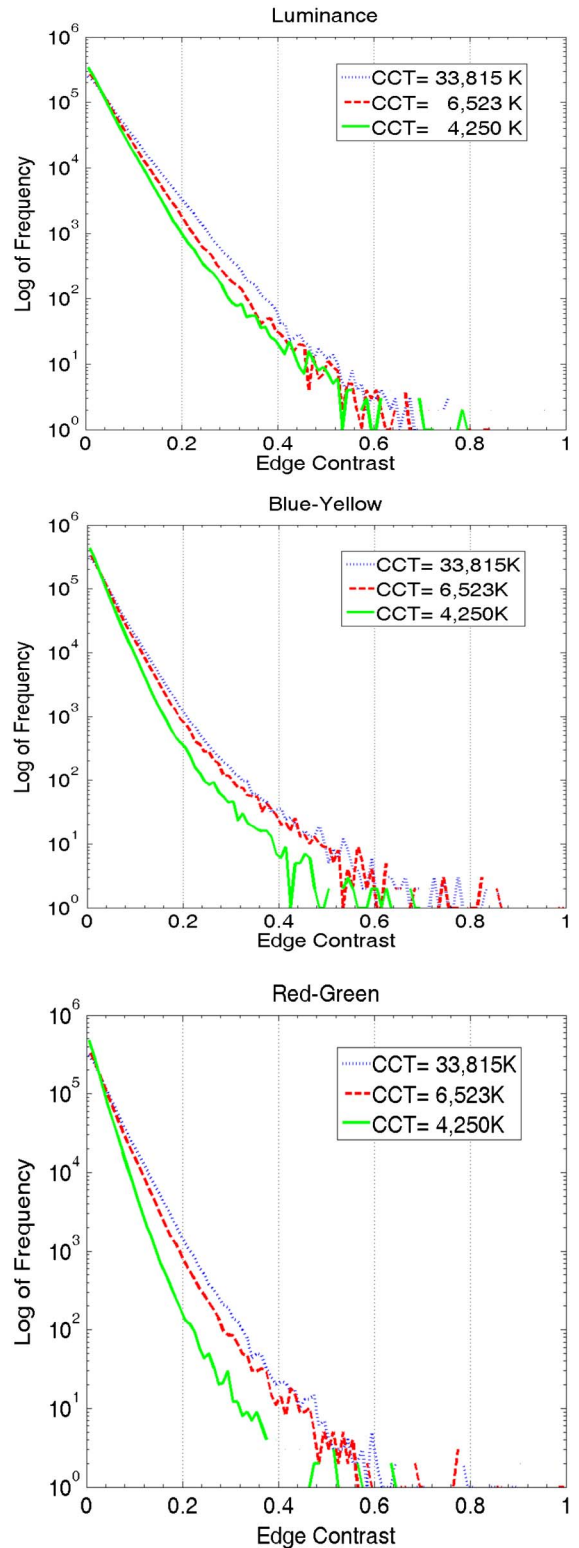


Fig. 3. (Color online) Example of the distributions of edge contrasts along the (a) nonopponent and (b)–(c) opponent color mechanisms for three daylights of different CCTs.

and this for color constancy [25]. If one of the major roles of the human visual system is to compensate for the illuminant changes (i.e., color constancy), how are edges processed by the color vision mechanisms to correct for the effects of natural illumination changes? To answer this question, cone

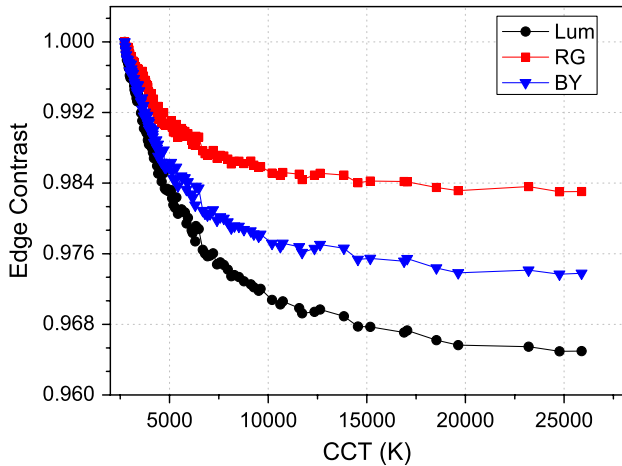


Fig. 4. (Color online) Normalized edge contrasts for the Lum, RG, and BY color mechanisms and natural daylights with correlated color temperatures ranging from 2735 to 25,889 K.

responses expressed by Eq. (1) should take into account adaptation. In the previous sections, we ignored any kind of adaptation-based cone excitations before the opponent responses and edge detection were evaluated.

Thus, to illustrate how natural illuminant changes influence the edge detection after adaptation, we also used a modified version of the previously used principal axes based on the following adapted receptor responses [20]:

$$\begin{aligned} L_R &= \log L - \overline{\log L}, \\ M_R &= \log M - \overline{\log M}, \\ S_R &= \log S - \overline{\log S}, \end{aligned} \tag{7}$$

where  $\log L$ ,  $\log M$ , and  $\log S$  are log pixel cone excitations and the upper bars represent the average of the corresponding log values for each image. Thus the three postreceptoral responses to each pixel will be

$$\begin{aligned} \text{Lum}_R &= L_R + M_R \\ \text{RG}_R &= L_R - M_R \\ \text{BY}_R &= 2S_R - (L_R + M_R), \end{aligned} \tag{8}$$

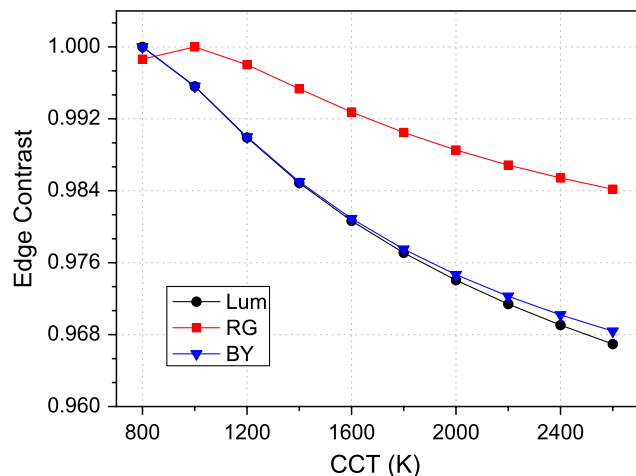


Fig. 5. (Color online) Normalized edge contrasts for the Lum, RG, and BY color mechanisms and Planckian illuminations with correlated color temperatures ranging from 800 to 2700 K.

where  $\text{Lum}_R$ ,  $\text{RG}_R$ , and  $\text{BY}_R$  are now the modified version of the color vision mechanisms represented by Eq. (2). The log version of the postreceptoral Lum, RG, and BY responses clearly takes into account local cone light adaptation. The logarithmic transformation will improve the coordinate spatial representation of cone responses and capture the fact that cone adaptation is local and as a result can produce spurious color signals. It can also take into account visual psychophysics because it is well known that uniform logarithmic changes in stimulus intensity tend to be equally detectable.

Following on from these transformations the edge detection and edge contrast were computed through Eqs. (3–6). Results suggest that edge contrast changes were apparently more stable with changes in daylight, except for some illuminations, as Fig. 6 shows. There were still slight deviations for low CCTs due to the logarithmic and differences calculations involved in Eq. (7) and the dark areas appearing in several of the hyperspectral images used. Thus, we cannot conclude that those modified color vision mechanisms were more optimally adapted to compensate for daylight changes in color edge detection than the unadapted postreceptoral systems used previously. What is clear again is that there is no optimal daylight CCTs to account for chromatic and luminance edge contrasts.

#### 4. GENERAL DISCUSSION

We have presented an analysis on how natural illumination influences the detection of color edges in natural scenes. Average statistics for edge differences among all possible pair of daylight illuminations suggest that, as daylight changes, chromatic and luminance edges also change, but only by a few percent. Spatial and temporal edges changes in natural illumination, with no differences among the postreceptoral responses to those changes. The average chromatic and luminance edge contrasts also change as daylight changes and the effect seems to be particularly relevant only for some color temperatures below 10,000 K where edge contrasts change abruptly but not dramatically. The edge contrast change was only 2% on average of the maximum contrast obtained at the lowest CCT. Considering the vast range of daylight CCTs analyzed, the edge contrast change rate is probably not visually

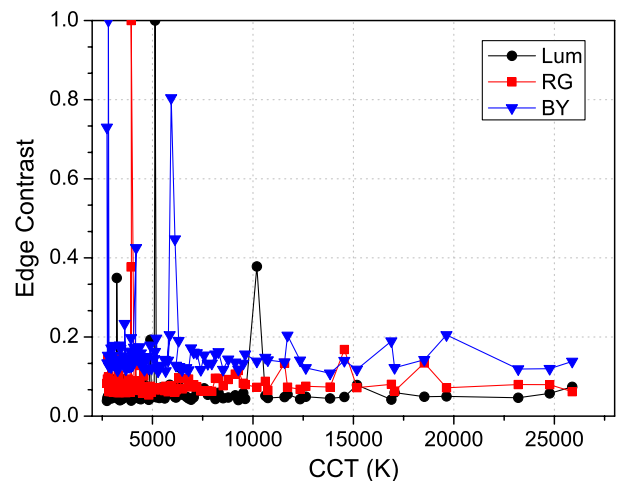


Fig. 6. (Color online) Normalized edge contrasts obtained using adapted receptor responses to derive the Lum, RG, and BY color mechanisms for different natural daylights.

relevant. This fact raises the question of how coding of luminance, color, and contrast is performed in the human visual system. Neurons in the visual cortex are expected to be tuned simultaneously to both chromatic and luminance contrasts. But this does not mean that color is made redundant by considering change relations rather than point intensities [10].

Previous work (e.g., [12]) found that the BY opponent channel varies with changes in daylight more acutely than the RG opponent response. The latter was almost constant across sunlight during a day but the BY response varies more than 40% from the minimum to the maximum activation at sunset, which means around 27% of contrast activation (i.e., contrast derived from the relationship between the difference of maximum and minimum values and the sum of both values from Fig. 4(b) in [12]). Even computing detection scores of fruits and foliage at different times of a day, the BY opponent system changes markedly at least for primates. As suggested by Lovell *et al.* [12], primates cannot take advantage of the separation of  $L$  and  $M$  cones, and thus the BY system is much more confounded by the natural illumination than the RG one. On the contrary, we found that color edge contrast changes change so little in comparison with the contrast activation for fruit and leaves detection. Our results suggest that there can be tasks (e.g., color edge detection) for which both opponent RG and BY systems are of “same quality,” even under dramatic daylight changes.

In addition to removing redundant information from the image, the receptor and postreceptor mechanisms adapt to natural illumination by stabilizing perceived color under different spectral light sources. What will be the implications if other non-log-transformed cone contrasts are used? A number of studies approach this problem by using definitions of RG and BY that either normalize the cone responses on a pixel-by-pixel basis [21,26], or by using log-transformed cone responses [20,27]. One could, for example, have used non-log-transformed cone contrasts, e.g.,  $L/Lm-M/Mm$  for the RG response, with  $Lm$  and  $Mm$  being the mean cone responses across the scene. The problem with this metric is that it does not account for the fact that cone adaptation is local and as a result can produce spurious color signals.

It should point out that our edge contrast definition does not take into account some properties of the human visual system. One limitation of our analysis is the influence of the neural noise in the edge contrast computation. The noiseless assumption followed in this work could be unnatural and should be discussed further. On one hand, we avoided consideration of noise in the study as an undue complication to our treatment. Throughout the computations, we assumed that the measures were taken in high photopic luminance levels along a day avoiding twilight. There are some works expressing that, at high intensities, the visual physical limit is dominated not by the quantum nature of light but by inefficiency in neural processing [28]. But these errors would not be noticeable in our study. On the other hand, to reliably estimate noise levels, it is necessary to assume a more physiological approach for the data and a particular accurate receptor integration time. Thus, visual judgments based on the selected cone signals will be reliable only under conditions of high photoreceptor signal-to-noise ratios or with considerable spatiotemporal averaging.

## ACKNOWLEDGMENTS

This work has been supported by the regional government of the Junta de Andalucía (Spain) through grant P07-TIC-02642. We are grateful to Shahram Peyvandi for his invaluable help and to the anonymous reviewers for helpful comments and suggestions.

## REFERENCES

- H. B. Barlow, “Possible principles underlying the transformation of sensory messages,” in *Sensory Communication* (MIT, 1961), pp. 217–234.
- E. P. Simoncelli and B. A. Olshausen, “Natural image statistics and neural representation,” *Ann. Rev. Neurosci.* **24**, 1193–1216 (2001).
- J. Hernández-Andrés, J. Romero, J. L. Nieves, and R. L. Lee, Jr., “Color and spectral analysis of daylight in southern Europe,” *J. Opt. Soc. Am. A* **18**, 1325–1335 (2001).
- Commission Internationale de l’Eclairage (CIE), Standard S 003/E-1996, *Spatial Distribution of Daylight—CIE Standard Overcast Sky and Clear Sky* (CIE, Vienna, 1996), p. 3.
- R. L. Lee, Jr. and J. Hernández-Andrés, “Colors of the daytime overcast sky,” *Appl. Opt.* **44**, 5712–5722 (2005).
- A. Hyvarinen, J. Hurri, and P. O. Hoyer, *Natural Image Statistics: A Probabilistic Approach to Early Computational Vision* (Springer, 2009).
- W. S. Geisler, “Visual perception and the statistical properties of natural scenes,” *Ann. Rev. Psychol.* **59**, 167–192 (2008).
- S. K. Shevell and F. A. A. Kingdom, “Color in complex scenes,” *Ann. Rev. Psychol.* **59**, 143–166 (2008).
- C. Zhou and B. W. Mel, “Cue combination and color edge detection in natural scenes,” *J. Vis.* **8**(4), 4, 1–25 (2008).
- T. Hansen and K. R. Gegenfurtner, “Independence of color and luminance edges in natural scenes,” *Vis. Neurosci.* **26**, 35–49 (2009).
- P. Sumner and J. D. Mollon, “Chromaticity as a signal of ripeness in fruits taken by primates,” *J. Exp. Biol.* **203**, 1987–2000 (2000).
- P. G. Lovell, D. J. Tolhurst, C. A. Parraga, R. Baddeley, U. Leonards, J. Troscianko, and T. Troscianko, “Stability of the color-opponent signals under changes of illuminant in natural scenes,” *J. Opt. Soc. Am. A* **22**, 2060–2071 (2005).
- R. M. Balboa and N. M. Grzywacz, “Occlusions and their relationship with the distribution of contrasts in natural images,” *Vis. Res.* **40**, 2661–2669 (2000).
- S. M. C. Nascimento, F. Ferreira, and D. H. Foster, “Statistics of spatial cone-excitation ratios in natural scenes,” *J. Opt. Soc. Am. A* **19**, 1484–1490 (2002).
- D. H. Foster, S. M. C. Nascimento, and K. Amano, “Information limits on neural identification of coloured surfaces in natural scenes,” *Vis. Neurosci.* **21**, 331–336 (2004).
- D. H. Foster, K. Amano, S. M. C. Nascimento, and M. J. Foster, “Frequency of metamerism in natural scenes,” *J. Opt. Soc. Am. A* **23**, 2359–2372 (2006).
- P. Ricchiazzi, S. Yang, C. Gautier, and D. Sowle, “SBDART: a research and teaching software tool for plane-parallel radiative transfer in the earth’s atmosphere,” *Bull. Am. Meteorol. Soc.* **2101**–2114 (1998).
- V. C. Smith and J. Pokorny, “Spectral sensitivity of the foveal cone photopigments between 400 nm and 500 nm,” *Vis. Res.* **15**, 161–171 (1975).
- R. L. DeValois and K. K. DeValois, “A multi-stage color model,” *Vis. Res.* **33**, 1053–1065 (1993).
- D. L. Ruderman, T. W. Cronin, and C.-C. Chiao, “Statistics of cone responses to natural images: implications for visual coding,” *J. Opt. Soc. Am. A* **15**, 2036–2045 (1998).
- C. A. Parraga, G. Brelstaff, T. Troscianko, and I. R. Moorehead, “Color and luminance information in natural scenes,” *J. Opt. Soc. Am. A* **15**, 563–569 (1998).
- G. R. Cole, T. Hine, and W. McIlhagga, “Detection mechanisms in  $L$ -,  $M$ -, and  $S$ -cone contrast space,” *J. Opt. Soc. Am. A* **10**, 38–51 (1993).
- M. Gazzaniga, *The New Cognitive Neurosciences*, 2nd ed. (MIT, 2000).

24. D. H. Foster, "Color constancy," *Vis. Res.* **51**, 674–700 (2011).
25. J. Golz and D. I. A. MacLeod, "Influence of scene statistics on color constancy," *Nature* **415**, 637–640 (2002).
26. Y. Y. Zeevi and S. S. Mangoubi, "Noise suppression in photoreceptors and its relevance to incremental intensity thresholds," *J. Opt. Soc. Am.* **68**, 1772–1776 (1978).
27. A. P. Johnson, F. A. A. Kingdom, and C. L. Baker, Jr., "Spatiochromatic statistics of natural scenes: first- and second-order information and their correlational structure," *J. Opt. Soc. Am. A* **22**, 2050–2059 (2005).
28. I. Fine, D. I. A. MacLeod, and G. M. Boynton, "Surface segmentation based on the luminance and color statistics of natural scenes," *J. Opt. Soc. Am. A* **20**, 1283–1291 (2003).